TISSUE ENGINEERING: Part A
Volume 17, Numbers 3 and 4, 2011

DOI: 10.1089/ten.tea.2010.0264

# Apatite Microtopographies Instruct Signaling Tapestries for Progenitor-Driven New Attachment of Teeth

Smit J. Dangaria, Ph.D. (Cand.),[1,2] Yoshihiro Ito, D.D.S.,[1] LeiLei Yin, Ph.D.,[3] Giovanni Valdré, M.Phil., Ph.D.,[4] Xianghong Luan, M.D.,[1] and Thomas G.H. Diekwisch, D.M.D., Ph.D. (sc.), Ph.D. (phil.)[1,2]

Dimension and structure of extracellular matrix surfaces have powerful influences on cell shape, adhesion, and gene expression. Here we show that natural tooth root topographies induce integrin-mediated extracellular matrix signaling cascades in tandem with cell elongation and polarization to generate physiological periodontium-like tissues. In this study we replanted surface topography instructed periodontal progenitors into rat alveolar bone sockets for 8 and 16 weeks, resulting in complete reattachment of tooth roots to the surrounding alveolar bone with a periodontal fiber apparatus closely matching physiological controls along the entire root surface. Displacement studies and biochemical analyses confirmed that progenitor-based engineered periodontal tissues were similar to control teeth and uniquely derived from preimplantation green fluorescent protein (GFP)-labeled progenitors. Together, these studies illustrate the capacity of natural extracellular surface topographies to instruct progenitor cell populations to fully regenerate complex cellular and structural morphologies of tissues once lost to disease. We suggest that our strategy could be used for the replantation of teeth lost due to trauma or as a novel approach for tooth replacement using tooth-shaped replicas.

## Introduction

The relationship between cells and their surrounding matrices is a partnership of mutual reciprocity. As much as cells control the shape and structure of extracellular matrices (ECMs) by complex secretory processes, these scaffolds in turn exert profound control over gene expression profiles and lineage commitment of stem cell populations.[1] Through topographical cues, scaffolds affect essential parameters of cell behavior, including cell adhesion, morphology, viability, apoptosis, and motility.[2] In recent years, the ability of natural ECMs to aide whole organ regeneration has become increasingly important.[3] While most natural ECM scaffolds rapidly disintegrate once removed from the body, the mineralized matrices of bones and teeth remain intact, often for hundreds or thousands of years after the surrounding organism is deceased. On a microenvironmental scale, the surface of these inorganic biological minerals retains a topographic impression of the cells and proteins that once contributed to their formation and contour, providing retrospective witness to the molecular interactions that helped to shape them.

Tooth root surface-mineralized tissue topography is affected by the shape of the cells that form the root surface (cementoblasts) and by the insertion sites for the fibers that provide the mechanosensory link between the tooth root surface and the alveolar bone socket (Sharpey's fibers). The host tissue for Sharpey's fibers at the interface between root surface and alveolar bone is a fiber-rich connective tissue called the periodontal ligament (PDL). The PDL not only contains Sharpey's fibers but also provides a multifunctional ECM environment for mechanosensation, signal transduction, shock absorption, and tissue remodeling. The periodontal ECM is rich in collagen, fibronectin, tenascin, periostin, and other matrix molecules.[4,5] Collagen I is the principal protein component of Sharpey's fibers[6] and periostin is an indicator molecule of a functional PDL, as its expression changes dynamically in response to tension and compression.[7] Other periodontal glycoproteins such as fibronectin and tenascin provide arginin-glycine-aspartic acid (RGD) motifs for cell adhesion.[8] Among these, fibronectin is also a key molecule involved in integrin signaling, cell–ECM attachment, cytoskeletal organization, and transduction of mechanical and chemical cues.[9] As much as the cells of the PDL control the deposition and remodeling of the ECM, the periodontal matrix also affects PDL cell behavior, and it is this reciprocity that provides the focus for the present application in tissue regeneration.

[1]Brodie Laboratory for Craniofacial Genetics, University of Illinois at Chicago, Chicago, Illinois.
[2]Department of Bioengineering, University of Illinois, Chicago, Illinois.
[3]Department of Microscopy Core, University of Illinois at Urbana Champaign, Urbana, Illinois.
[4]Laboratory of Biomaterials and Applied Crystallography, Department of Earth Sciences, University of Bologna, Bologna, Italy.

To utilize the unique surface properties of mineralized tooth roots for tissue regeneration, we are now taking advantage of the inorganic memory of past cell–matrix interactions. To illustrate the instructive capacity of tooth root cementum, we have exposed the unique surface topography of denuded tooth roots to instruct tissue-specific differentiation of periodontal progenitor cells. Our findings indicate that root cementum surface topographies induce highly specific integrin-mediated ECM signaling cascades, which in turn restore periodontal progenitor populations into periodontal tissues genetically and functionally matching those of their natural counterparts. Moreover, our technique of replanting denuded tooth roots seeded with periodontal progenitors proved to be an effective strategy to fully regenerate lost tooth periodontia.

## Materials and Methods

The present study begins with a number of *in vitro* experiments that establish the relationship between tooth root surface topography, initial cell attachment, and focal adhesion, followed by *in vitro* feasibility studies demonstrating mouse PDL progenitor cell (mPDLP) attachment on micropatterned apatite surfaces. The remaining part of the study is dedicated toward our progenitor-populated tooth root replantation model and its biological verification (Table 1).

### *mPDLP cell culture and green fluorescent protein labeling*

First mandibular molars of CD-1 mice were extracted and PDL attached to root surfaces was scraped off. Tissue scrapings were then digested to release singles cells that were further cultured to give rise to colonies. Cell clones (colonies) with the highest ability to differentiate into osteogenic, adipogenic, and chondrogenic lineages were used as progenitor cells in subsequent experiments. For stable expression of green fluorescent protein (GFP), mPDLPs were transduced with plasmid Babe (pBabe)-eGFP retroviral vector kindly gifted by Nissim Hay as described previously.[10]

### *Scanning electron microscopic analysis of mPDLPs cultured on nano-hydroxyapatite, microporous root, and smoothened root surfaces*

mPDLPs were seeded and cultured for 6 h on 3 $mm^3$ blocks of nano-hydroxyapatite blocks (nano-HA), ethylenediaminetetraacetic acid (EDTA)-etched tooth root surface (microporous root) of rat maxillary first molars, or on artificially smoothened root surface created by polishing. Alternately, mPDLPs were seeded on EDTA-etched tooth roots and either cultured for 3 days and then replanted back in the corresponding tooth socket for 8 and 16 weeks or left in culture *in vitro* for 10 days. Noncell-seeded tooth roots served as the controls in both sets of experiments. After the stipulated time points, samples were fixed, dried, splutter coated with gold-pallidium, and viewed using a 3500-S Hitachi scanning electron microscope.

### *Characterization of surface topography and cell attachment and spreading on implant surfaces*

Surface topography parameters such as amount and size of pores on nano-HA, microporous tooth root, and smoothened root surface were calculated by measuring pore sizes (mean diameter) on scanning electron micrographs of these surfaces using the NIH imaging software (ImageJ), and values were reported as percentages of pore sizes in the range of (5–100 nm) on nano-HA and (50–400 μm) on microporous root surface. Cell spreading on nano-HA, microporous root surface, and smooth root surface after 6 h of incubation was measured in terms of cell elongation, which was calculated as a ratio of cell length to width.

### *Osteogenic, adipogenic, and chondrogenic differentiation of mPDLPs*

For osteogenic differention, mPDLPs were seeded at 3500 cells/$cm^2$ and cultured in Differentiation Basal Medium-Osteogenic medium (Lonza) and maintained for 21 days. Osteogenic mineralization nodules were assessed with Alizarin Red S staining. For chondrogenic differentiation, about $5\times10^5$ mPDLPs were pelleted down in a 15 mL polypropylene tube and cultured in Differentiation Basal Medium-Chondrogenic (Lonza) supplemented with 10 ng/mL TGF-B3 and maintained for 21 days. The medium was changed every 3 days. After 21 days of culture, pellets were formalin fixed and paraffin embedded, and 5 μm section were cut and immunostained with collagen type II antibody to assess chondrogenic differentiation. For adipogenic differentiation, about $2.5\times10^5$ mpDLPs were plated into each well of a six-well plate. The cells were subjected to three cycles of adipogenic induction/maintenance starting at confluence. Each cycle involved treating the mPDLPs with

Table 1. Study Design

*In vitro* studies establishing the relationship between tooth root surface topography, initial cell attachment, and focal adhesion (Fig. 1)
*In vitro* feasibility studies demonstrating attachment of mouse periodontal ligament progenitor cells on root surfaces of extracted teeth (Fig. 2)
*In vivo* replantation of periodontal progenitor-populated tooth roots into tooth molar sockets (Figs. 3–5)
- Clinical evaluation in animals
- Histology
- Microcomputed tomography
- Scanning electron microscopy
- Mechanical function test
- Recognition of GFP-labeled progenitors in replanted tissues
- Molecular characterization by immunohistochemistry and Western blot

GFP, green fluorescent protein.

adipogenic induction medium for 3 days followed by adipogenic maintenance medium for the next 3 days. At the end of 21 days of culture, mature adipocytes were detected by Oil Red O staining. Adipogenic, osteogenic, and chondrogenic differentiation media were purchased from Lonza.

### In vitro *culture of mPDLPs, dental follicle progenitors, dental pulp, and MC3T3 cells on microstructured HA chips*

To observe the attachment behavior of odontogenic cells to HA surfaces about $1\times10^6$ mPDLPs, dental follicle progenitors, dental pulp, and nonodontogenic preosteoblasts MC3T3 cells were suspended in 200 μL of Dulbecco's modified Eagle's medium and incubated on top of HA chips 1-mm-thick placed in a well of a six-well plate for 2 h. After washing out unattached cells with phosphate-buffered saline (PBS), HA-cell constructs were cultured for 3 days and cell attachment pattern on and around HA chips were observed using phase-contrast microscopy.

### *First maxillary molar extraction and subsequent replantation*

All animal procedures were approved by and complied with the guidelines provided by the Institutional and Animal Care and Use Committee at the University of Illinois, Chicago. Eighteen athymic nude rats (approx. 250 g, body weight) were fed powdered rat chow containing 0.4% beta aminopropionitrile for 2 days to reduce the tensile strength of collagen molecules and to facilitate gentle tooth extraction with minimum damage to the surrounding periodontal tissues.[11] Under anesthesia with ketamine (100 mg/kg)/xylazine (5 mg/kg), first maxillary molars were extracted using forceps, and subjected to collagenase/dispase treatment to digest the attached PDL fibers and cells. The denuded teeth were then treated with 5% EDTA solution pH 7.4 for 10 min (surface demineralization and exposure of organic matrix), washed thoroughly with distilled water, and fixed in 70% ethanol overnight. Tooth samples were then washed thoroughly in Dnase/Rnase-free water for 4 h with three changes to fresh water and air-dried in a sterile hood to prepare for cell seeding. Immediately after extraction, the sites were cleaned with surgical dental burs, plugged with a collagen sponge, and allowed to heal until replantation. The extraction sites were reopened after 4 days of healing, and cleaned with a dental bur under constant irrigation to facilitate easy reentry of the extracted maxillary molars. Molars used for replantation were either seeded with mPDLPs and cultured for 3 days or left untreated. Once the tooth was replanted back in its socket, it was stabilized with the adjacent second molar using a thin coat of glass ionomer dental restorative just high enough to maintain the physiologic occlusion with the corresponding mandibular molar. In all a total of 36 molars were replanted back in their respective tooth socket; 14 of them were cell-free replants and the remaining 22 were seeded with mPDLPs before replantation.

### *Masson's Trichrome staining*

mPDLPs were seeded on EDTA-etched first molars and either cultured *in vitro* for 3 days before replantation into the corresponding healing tooth socket for 8 weeks or left in culture for 10 days. Noncell-seeded molars served as the controls. At the end of the stipulated time point for *in vitro* and *in vivo* studies the implants were harvested, fixed, decalcified, and processed for paraffin embedding. Subsequently, 5-μm-thick sections were stained with Masson's trichrome stain (Sigma).

### *Micro-computed tomography analysis*

To observe mineralized tissues, maxillary tissue blocks with replanted teeth with or without mPDLP treatment were analyzed using microcomputed tomography (micro-CT). For this purpose, 3D X-ray CT images were acquired by means of an Xradia MicroXCT 400 (Xradia). Briefly, a 1024 by 1024 image matrix size over a 5.12 mm field of view was used to create an isotropic voxel size of 5 μm. A total of 1024 slices were acquired for each tooth section. No filtering processes were applied after the scan and reconstruction. During the scans, 30 keV 6 watt X-ray beam were generated to image the samples; 5 s exposure time was used for each of the hundreds of projection images with 0.25° step angle.

### *Immunohistochemistry and -fluorescence*

Rat maxillae with mPDLP-seeded replanted teeth and noncell-seeded replanted teeth 8 weeks after replantation in the tooth socket were harvested, fixed, decalcified, and processed for paraffin embedding and sectioning. In another study, mPDLPs were seeded on fibronectin-coated cover slips with integrin α5β1 blocked or unblocked and cultured for 12 h *in vitro*. The effect on actin stress fiber formation was observed using rhodamine conjugated phalloidin. For immunohistochemistry, slides were deparaffinized and tissues were rehydrated. Immunoreactions were performed as previously described,[12] using monoclonal primary antibody for periostin (Abcam), bone sialoprotein (BSP) (Abcam), and GFP on both the mPDLP-seeded experimental group and the noncell-seeded control groups. Sections were incubated with primary antibody at room temperature for 1 h at a dilution of 1:500 in PBS. Sections were washed and incubated for 10 min with appropriate anti-mouse IgG or anti-rabbit IgG secondary antibody and further incubated with streptavidin-enzyme conjugate. Signals for immunoreactions were detected using 3-amino-9-ethylcarbazole (AEC) substrate–chromogen mixture (color substrate) and counterstained with hematoxylin, and slides were mounted using glycerol vinyl alcohol aqueous (GVA) mount. For negative controls, the primary antibody was replaced with a similar amount of PBS.

### *Mechanical testing of functional tooth reattachment*

After 16 weeks of replantation, mPDLPs seeded and noncell-seeded control groups were harvested with the teeth intact in the maxilla and subjected to mechanical testing using a Wagner force dial gauge (Wagner instruments, Inc.). The rat head was held firmly in place using a metal clamp. A metal probe was designed to apply translational force to the crowns of the replanted teeth (both mPDLP-seeded experimental group and noncell-seeded controls) and the amount of displacement was then captured using a digital camera. Tooth crown surfaces were subjected to both 10 and 15 N translational force, with the exception of loosely attached teeth from the noncell-treated replant group, in which case on 1 N was applied. At each force levels, three measurements were obtained and the amount of displacement was recorded

in each case. The images were captured before and after the application of force and the net displacement of the first maxillary molar was calculated as a difference between the position of a reference point on the first molar in relationship to the image midline before force application and the position of the same reference point related to the image midline after application of the force.

*Western blot analysis*

mPDLPs were cultured on nano-HA, artificially smoothened tooth root, EDTA-etched tooth root surface, polished apatite, or roughened apatite for 6 h to observe initial cell attachment. Alternatively, mPDLPs were seeded on EDTA-etched denuded tooth roots for 3 days before replantation in

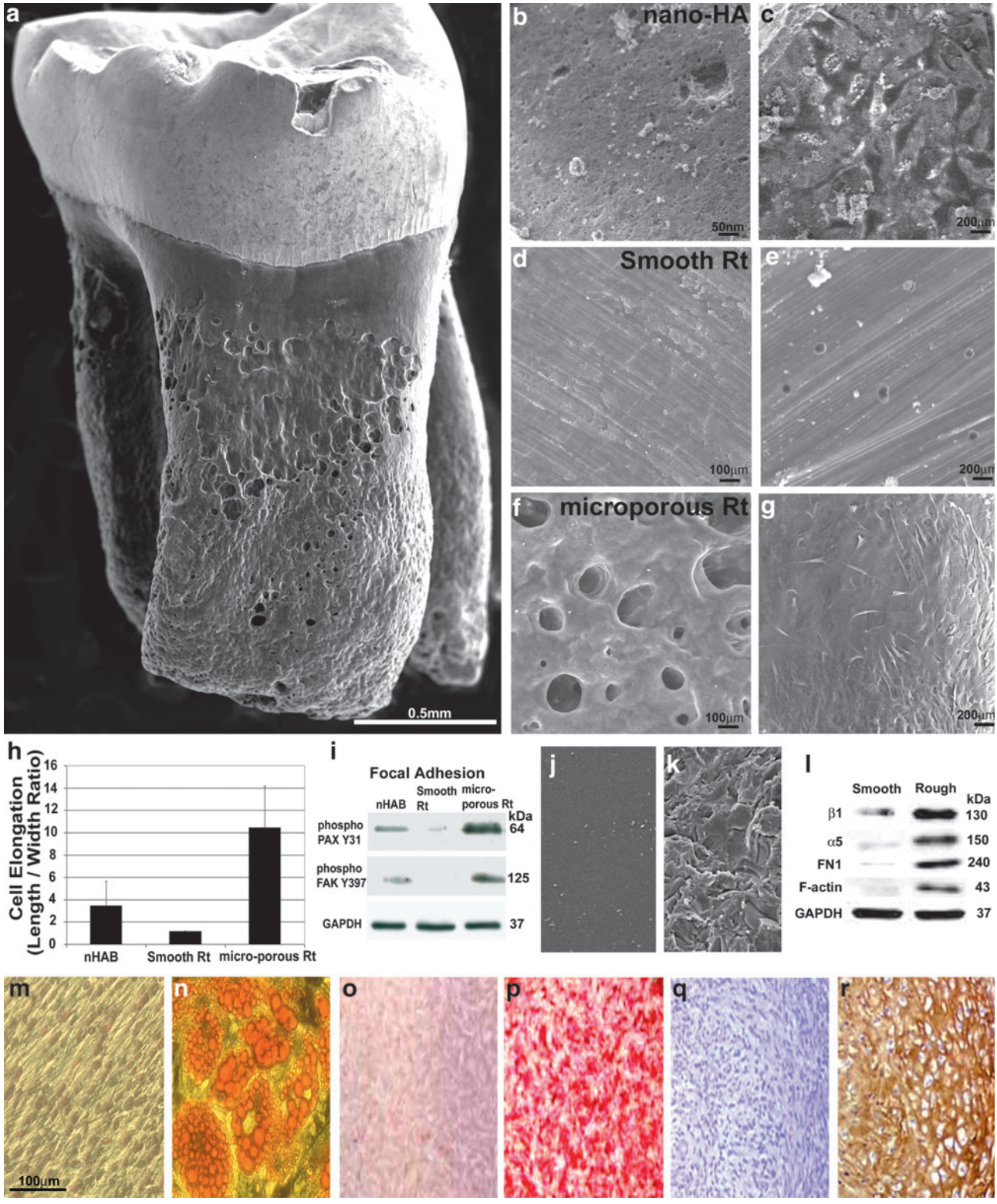

the tooth socket or cultured in 2D on tissue culture plastic. Progenitor cell-seeded teeth and noncell-seeded controls were replanted in the tooth socket for 8 weeks. At the end of each experimental time point, samples were harvested and washed with PBS. The constructs were then homogenized in sodium dodecylsulfate-polyacrylamide gel electrophoresis sample buffer and proteins extracted as described.[10] Identical amounts of protein extracts from all experimental and control groups were separated on a 4%–20% sodium dodecylsulfate-polyacrylamide gel electrophoresis gel and transferred to polyvinylidene fluoride membrane in a semi-dry blotting apparatus containing transfer buffer (25 mM tris, 40 mM glycine, 10% methanol) for 45 min at 75 mA. The polyvinylidene fluoride membrane was then blocked with 5% bovine serum albumin for 1 h at room temperature and the blot was incubated with 1:1000 dilution of periostin, tropoelastin, tenascin-C, fibronectin, collagen type II, Rho A (1:2000), F-actin (1:700), integrin α5 (1:1500) and β1 (1:1500), and glyceraldehyde 3-phophate dehydrogenase (1:2500) (all from Abcam) antibodies for 2 h, washed with TBST three times and incubated with 1:2500 dilution of HRP-conjugated anti-rabbit or anti-mouse secondary antibody, respectively (Zymed), for 1 h, and further washed three times with TBST. HRP was detected using a chemiluminescent substrate (Supersignal West Pico Chemiluminescent Substrate; Pierce).

### *Statistical analysis*

All experiments were performed in triplicate unless stated otherwise. Final values were reported as means ± standard deviation. Data were analyzed using Student's *t*-test and *p*-values $< 0.005$ in each comparison were considered statistically significant.

## Results

### *Natural tooth root surfaces are microporous*

The fully developed rodent molar tooth root features an intriguing surface structure of microporosities, ridges, and impressions (Fig. 1a). Further analysis of an EDTA-etched native rat molar root surface compared with nano-HA block (Fig. 1b) and an artificially smoothened root surface (Fig. 1d) revealed pores between 50 and 400 μm in diameter on native root surfaces, whereas artificially smoothened root surfaces did not contain measurable pores and nano-HA contained pores from 5 to 100 nm in diameter (Fig. 1b, d, f). To test the effect of surface pattern on cell behavior, mPDLPs were cultured on the aforementioned apatite surfaces for 6 h and cell dimensions were evaluated thereafter. After culture, cell length to width ratios were 3.56 on nano-HA surfaces, 1.05 on smoothened root surfaces, and 10.28 on naturally porous native root surfaces (Fig. 1c, e, g, h). In comparison, cells on naturally porous native root surface were 9.8-fold more elongated than those on smoothened root surfaces, whereas cells on nano-HA surfaces were less elongated (2.85-fold) than those residing on naturally porous native root surfaces ($p < 0.005$ for each comparison). We interpret these findings as a result of patterned surface topography to facilitate cell polarization.[13] These effects of apatite surface microtopography on cell behavior are also supportive of previous reports in other model systems, mostly osteoblasts and implant studies, all indicating that roughened microtopographies improve mineral deposition, adhesion, migration, proliferation, and osteogenic differentiation.[14–17]

### *Apatite surface morphology alters cell shape and early response gene expression*

On the basis of the intimate relationship between surface topography and cell adhesion behavior, we speculated that expression of key early focal adhesion mediators would be affected by surface properties. To test the effect of surface topography on cell adhesion machinery in periodontal progenitors, cells were once more incubated on different apatite surfaces for 6 h. In a first set of experiments we tested the effect of surface parameters on two early focal adhesion proteins involved in mediating cell–ECM contacts, paxillin (PAX) and focal adhesion kinase (FAK).[18] Compared to PDL progenitors cultured on nano-HA, mPDLPs on microporous natural root surfaces featured an 8.8-fold increase in phospho-PAX Y31 and a 6.2-fold increase in phospho-FAK Y397. In contrast, phospho-PAX Y31 on smoothened root surfaces was 8.3-fold reduced and phospho-FAK Y397 was not detectable (Fig. 1i). To assess to what extent the effects of surface properties on gene expression were solely due to surface properties, cells were incubated on rough and smooth apatite surfaces derived from an identical block of mineral. Surface roughness was modified either by polishing or by sandblasting in conjunction with steam cleaning (Fig. 1j, k). After 12 h of culture on these two surfaces, cells maintained a spherical shape on smooth surfaces in contrast to elongated

**FIG. 1.** Effect of tooth root surface topography on initial attachment and spreading of mPDLPs. Under the scanning electron microscope the natural root surface of a rat mandibular first molar exhibits an intricate, heavily grooved topography. The microporous topography of a ethylenediaminetetraacetic acid-etched root surface **(a, f)** had a significantly more pronounced surface relief than a nanostructured, nano-HA apatite surface **(b)** or a smoothened and polished root surface **(d)**. Differences in surface topography resulted in significant changes in cell shape and attachment when apatite surfaces were seeded with mouse periodontal progenitor cells. On nano-HA, cells were flattened and spread out **(c)**, on smoothened root surface apatite there was little or no attachment of cells **(e)**, and on a microporous root surface, cells demonstrated an elongated, fibroblast-like morphology **(g)**. Compared to mPDLPs grown on smooth or nano-HA surfaces, mPDLPs grown on microporous root surface apatite were significantly more elongated **(h)**. Western blots demonstrated that the two early attachment focal adhesion proteins phospho-paxillin Y31 and phospho-focal adhesion kinase Y397 were highly expressed on cells attached to microporous root surfaces, whereas expression of these adhesion proteins was reduced in cells on nano-HA surfaces and almost absent in cells cultured on smoothened apatite surfaces **(i)**. Changes in gene expression as a result of surface topography were not unique to native rat molar tooth roots but also occurred on smoothened or roughened apatite surfaces of identical chemical composition **(j–l)**. **(m–r)** Images document the multipotency of mPLDPs to differentiate toward adipogenic **(n)**, osteogenic **(p)**, and chondrogenic **(r)** lineages compared to noninduced negative controls **(m, o, q)**. mPDLP, mouse periodontal ligament progenitor cell; nano-HA, nano-hydroxyapatite; PAX, paxillin; FAK, focal adhesion kinase.

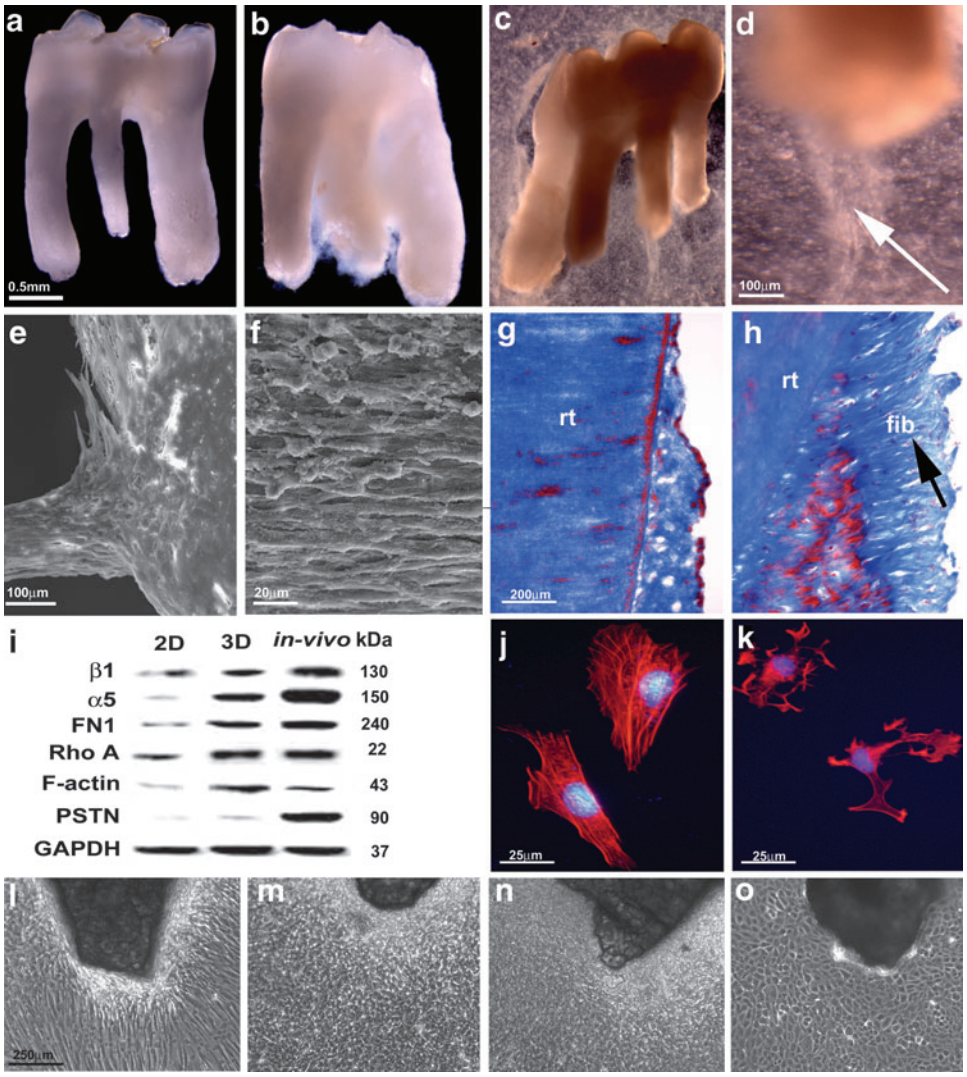


**FIG. 2.** Attachment and growth of mPDLPs on root surfaces of extracted teeth *in vitro.* **(b, c, d)** Light microscopic images of mPDLPs attached to denuded first maxillary molars and cultured *in vitro* for 3 days before replantation in the tooth socket. Note the extension of fiber bundles and progenitor cells at the apical tip of the cultured implant (arrow, **d**). **(a)** A denuded rat first maxillary molar before treatment with mPDLPs. **(e, f)** The distribution and morphology of mPDLPs seeded on rat first maxillary molars after 10 days of culture using scanning electron microscopy. Note the PDL-like fibrous outgrowth of parallel-aligned and elongated PDL-like cells at the apical end of the tooth root. Histological analysis revealed fibrous attachment (arrow, **h**) of mPDLPs on root surfaces after 10 days **(h)** compared to untreated controls **(g)**. Western blot **(i)** document significant changes in protein expression after PDL progenitors were exposed to micropatterned 3D surfaces. **(i)** Micropatterned 3D environments were created either by 3D cell culture in conjunction with micropatterned tooth root surfaces (center column: 3D) or after *in vivo* replantation for 8 weeks (right column: *in vivo*), and protein expression levels were compared to mPDLP expression levels in 2D culture without any microstructural challenge (left column: 2D). For all six proteins investigated (β1 integrin, α5 integrin, fibronectin, Rho A, F-actin, and periostin), protein levels were higher after exposure to 3D micropatterned root surfaces **(i)**. Integrin α5β1 blockage **(k)** resulted in a loss of actin fibers and polarization when compared to control mPDLPs cultured on fibronectin coated plates **(j)**. **(l–o)** Images compares various progenitor lineages and preosteoblast MC3T3 cells in response to microstructured surface topography. mPDLPs demonstrated highly elongated, fibroblast-like shaped cells aligned perpendicular to the microstructured apatite chips **(l)**, whereas dental follicle progenitors **(m)**, dental pulp cells **(n)**, and MC3T3 cells **(o)** formed small and polygonal cells surrounding the microstructured apatite chips. rt, root; fib, fibers; GAPDH, glyceraldehyde 3-phophate dehydrogenase; PSTN, periostin.

spindle shaped morphology on rough surfaces (data not shown). To determine the effect of surface roughness on cell attachment mediators, changes in fibronectin and related integrin cell surface mediators were assessed. Smooth apatite surfaces demonstrated a significant reduction in β1 and α5 integrin cell surface mediators (7.1-fold for β1 and 14.3-fold for α5) in tandem with similarly dramatic reduction in the fibronectin ECM protein (67.8-fold reduction) and the cytofilament F-Actin (101.3-fold) as shown by Western blot analysis (Fig. 1l) ($p < 0.005$ in each comparison). To verify the multipotent potential of mPDLPs, cells were induced with adipogenic, osteogenic, and chondrogenic differentiation media for a period of 21 days, resulting in lipid granules after adipogenic induction, Alizarin Red–stained calcium deposits after osteogenic induction, and collagen II expression after chondrogenic induction (Fig. 1m–r). Together, these studies demonstrate how simple modifications in apatite surface topography alone result in powerful alterations in mPDLP cell shape and in the expression of key early molecules involved in PDL progenitor cell adhesion to a substrate.

### *De-cellularized root surfaces induce periodontal progenitor polarization via integrin signaling pathways*

On the basis of the conduciveness of natural tooth root surfaces to trigger cellular elongation and expression of

molecular adhesion mediators as demonstrated in our first set of experiments, we asked whether de-cellularized and denuded surfaces of extracted teeth would provide a suitable microenvironment to stimulate attachment and tissue-specific growth of periodontal progenitor cell populations. To test whether extracted teeth would provide inductive scaffolds for mPDLPs, cells were grown on denuded tooth roots *in vitro* for either 4 or 10 days, and newly formed tissues were evaluated using scanning electron microscopy and histology. We found that after 4 days, mPDLPs formed a dense population of cells surrounding the incubated tooth root (Fig. 2a–d). After 10 days of incubation, the root surface was immersed into a dense lawn of cells and fibers (Fig. 2e, f, h). Histological investigation revealed cells and parallel-oriented fibers perpendicular to the root surface (Fig. 2h) on denuded and then mPDLP seeded first molars compared to an absence of fiber bundles on untreated surfaces (Fig. 2g). This striking effect of root surface haptotactic signals on PDL stretching and perpendicular fiber orientation resembles previous observations related to integrin-mediated cell polarization in other systems.[19,20]

On a molecular level, the extraordinary ability of cells to adjust their cytoskeletal organization, and hence their shape and motility, to minute changes in their immediate surroundings is accomplished by integrin-based adhesion complexes, which are tightly associated with the actin cytoskeleton.[21] To test the effect of integrin cell surface receptors on cell shape and cytoskeletal organization and since fibronectin is one of the major periodontal ECM proteins, we decided to focus on the two major fibronectin-associated integrin subunits α5 and β1, which are preferentially expressed to a higher extent in PDL cells.[22–26] To determine the effects of root surface topography on integrin-related signaling networks, we have compared mPDLPs exposed to regular 2D culture dishes (2D), 3D root surface environments *in vitro* (3D) (i.e., cells were grown *in vitro* on denuded root surfaces for 3 days before replantation), and mPDLPs that were replanted *in vivo* for 8 weeks (*in vivo*) (Fig. 2i). Compared to tooth-cell constructs implanted *in vivo*, α5 and β1 integrin expression was reduced to 50% in 3D cultures, whereas in 2D cultures expression levels were once more reduced to 34% (β1) and 6% (α5) (Fig. 2i). Surprisingly, F-actin expression in 3D culture was 2.32-times higher than comparable expression levels *in vivo*, whereas expression levels in regular 2D culture dishes was reduced to 37%. Rho-A was expressed at a similar level in 3D culture and in *in vivo* replants, and was reduced to 44% in 2D cultures compared to *in vivo* constructs. Periostin expression in 2D and 3D cultures was severely reduced to 2% and 15%, respectively, compared to *in vivo* replants (Fig. 2i). Together, these data indicate that exposure to topographically patterned 3D root surfaces greatly enhances protein levels of integrin α5 and β1, fibronectin, Rho A, and actin microfilaments (F-actin), both *in vitro* and *in vivo*. A possible exception to this trend was the periodontal ECM protein periostin, which was uniquely elevated in implanted periodontia, whereas exposure to cultured root surfaces (Fig. 2i) resulted only in a marginal increase in expression levels. This tissue-specific dependency of periostin on periodontal environments may be due to neighboring tissues or due to the effect of mechanical forces and stimuli that continuously affect the periodontium. Together, these data establish that the mineralized tooth cementum surface contains much of the instructive information required to trigger integrin-based focal adhesion events and subsequent cell polarization in periodontal progenitors.

Our studies subjecting mPDLPs to three-dimensional root surfaces or periodontal *in vivo* environments indicate that periodontal tooth root surface topography affects many molecules that are involved in classical integrin signaling cascades. Here we once more focused on α5 and β1 integrins. After blockage of α5 and β1 integrins using specific antibodies, periodontal progenitors lost their polarized orientation, developed processes, and assumed a polygonal overall shape (Fig. 2k). In addition, there was a significant loss of actin microfilament-related stress fibers (Fig. 2k), underscoring the pivotal role of integrins in the maintenance of cell shape and polarization. Cells cultured on fibronectin coated plates without integrin blockage showed intense stress fiber formation and a cell length to width ratio of 5.6 that was significantly higher than in cells in which integrins α5β1 were blocked and had a cell length to width ratio of only 1.15 (Fig. 2j, k). We then compared three different odontogenic progenitors (mPDLPs, dental follicle progenitors, and dental pulp cells) and preosteoblast MC3T3 cells, to ask whether formation of attachment tissues on apatite surfaces depended on surface structure alone. Our data document that mPDLPs formed highly elongated, fibroblast-like shaped cells aligned perpendicular to microstructured apatite surfaces, whereas dental follicle progenitors, dental pulp cells, and MC3T3 cells formed small and polygonal cells surrounding the microstructured apatite chips (Fig. 2l vs. m, n, o), demonstrating that formation of cellular fibrous tissues on apatite surface was not only dependent on surface topography but also on progenitor cell type. Together, these findings support our concept that integrin-based signaling cascades are involved in mPDLP polarization and gene expression changes that mediate the effects of tooth root surface properties on periodontal tissue differentiation and ECM fiber formation.

### *Successful replantation of denuded tooth scaffolds populated with periodontal progenitors*

The faithful reproduction of periodontal fiber formation and orientation on *in vitro* cultured, denuded root surfaces prompted us to ask whether mPDLP-populated, extracted, and denuded tooth matrices would provide suitable templates for the replantation of extracted teeth. To test this hypothesis, first maxillary rat molars were extracted, cleaned, and repopulated with periodontal progenitors. In tandem, rat molar extraction wounds were covered with a collagen sponge and allowed to heal for 4 days. After 4 days, extracted teeth repopulated with mPDLPs were replanted into extraction sockets, stabilized with glass-ionomer, and kept within the rat's mouth for 2–4 months. After 2 and 4 months, mPDLP-treated and replanted teeth were entirely integrated into the rat molar tooth row (Fig. 3b) and resembled wild-type (WT) control teeth (Fig. 3a). In contrast, only a portion of the non-mPDLP treated tooth replants remained in the jaw (Fig. 3c). Detailed analysis using histology (after 8 weeks), micro-CT, and scanning electron microscopy (after 16 weeks) revealed that the periodontal apparatus of the replanted tooth molar root consisted of cementum, alveolar bone, and a physiological PDL (Figs. 3e, h, j, k and 4a, c, d), resembling

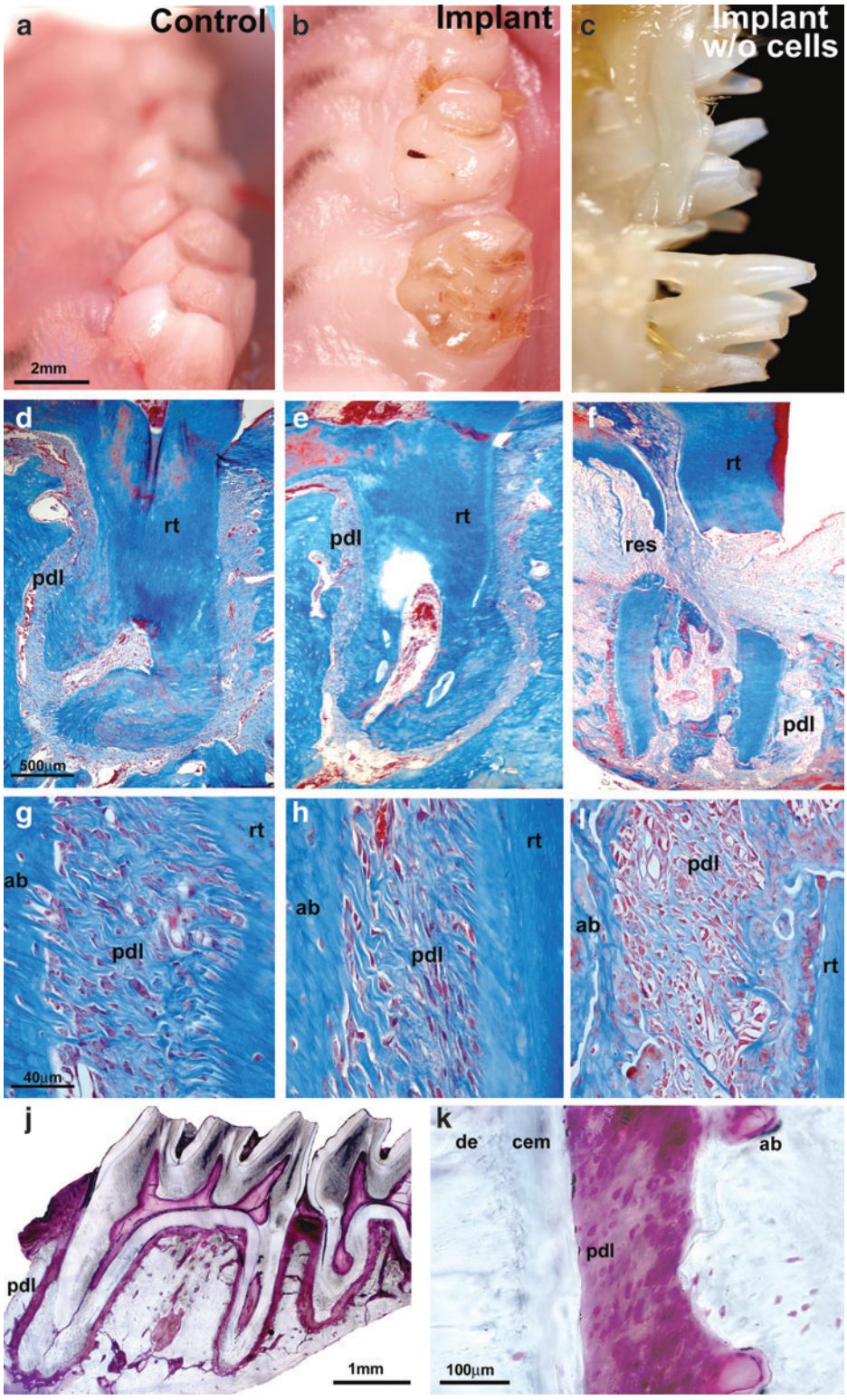


**FIG. 3.** Periodontal progenitor-driven new attachment of denuded teeth after 8 weeks of implantation in a tooth molar socket. Vertical columns: **(a, d, g)** WT controls; **(b, e, h)** replanted mPDLP-treated molars; and **(c, f, i)** replanted molars that were not treated with progenitor cells before replantation. Horizontal rows: **(a–c)** oral micrographs of rat upper right molar tooth rows; **(d–f)** overview histological preparations documenting the root surface/ligament interface of an entire upper first molar tooth root; and **(g–i)** detailed histological micrographs of the root surface/PDL/alveolar bone interface in all three groups. **(b, e, h)** Complete anatomical and histological integration of denuded and then mPDLP-treated rat first molars after 8 weeks of reimplantation. Reimplanted rat molars that were not subjected to progenitor cell reattachment were either lost, partially exfoliated **(c)**, or partially resorbed **(f, i)**. Our replantation approach resulted in the progenitor-based periodontal tissue engineering of the entire periodontium of a first maxillary molar **(j, k)**. **(j, k)** Ultrathin ground sections in which the periodontium was stained with fuchsin. **(j)** The background outside of the fixed tooth organ was digitally removed and no other alterations were applied to the micrograph. Individual tissues are labeled for orientation. de, dentin; cem, cementum; pdl, periodontal ligament; ab, alveolar bone; res, resorption site; rt, root; $m_1$, first maxillary rat molar. WT, wild type.

the PDL of control molar roots (Fig. 3d, g). Ground sections of progenitor-treated and replanted molar teeth demonstrated that this procedure resulted in the new formation of the entire PDL of a multirooted tooth with physiological new fiber attachment on two molar tooth roots (Fig. 3j). In contrast, tooth molars that were replanted without prior incubation in periodontal progenitor cell lawns were either lost entirely, partially exfoliated, ankylosed, or extensively resorbed (Figs. 3c, f, I and 4b, e, f). Among the 14 cell-free replants, 28.5% of the molars were lost, 21.4% were ankylosed, and about 50% were loosely attached (Fig. 4g). Eight and 16 weeks after replantation surgery all of the 22 molar tooth replants treated with progenitor cells were firmly attached to their corresponding tooth socket.

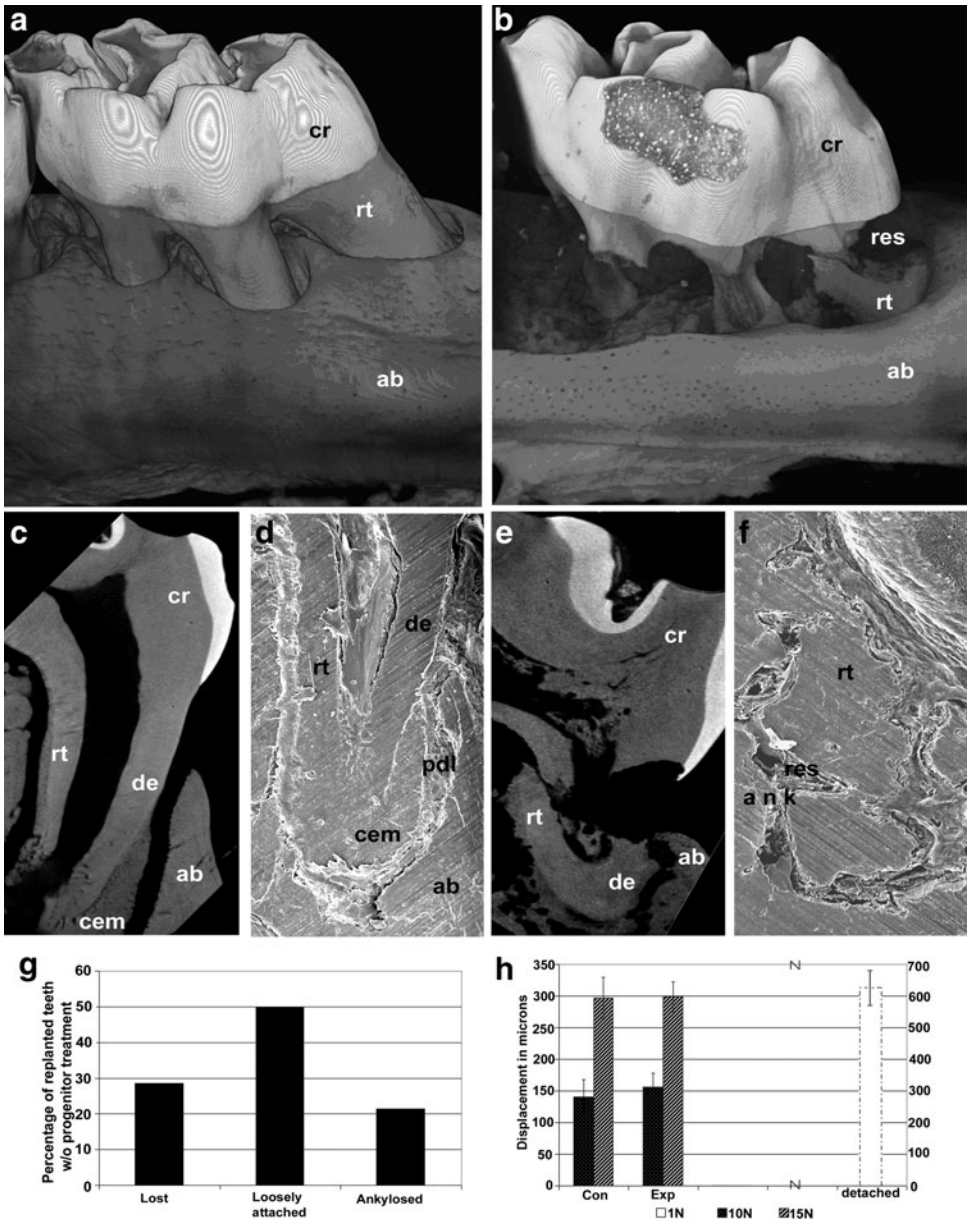


**FIG. 4.** Micro-CT, scanning electron microscopic analysis, and mechanical functional test of progenitor cell-treated reimplanted teeth versus replants without progenitor cell pretreament. **(a, b)** 3D-reconstructed micro-CT images of replanted rat molars that were either repopulated with periodontal progenitors **(a)** or left untreated **(b)** after 16 weeks of replantation. **(c–f)** Higher magnification micro-CT sections **(c, e)** or scanning electron micrographs **(d, f)** of a single first molar mesial root from progenitor-treated **(c, d)** and untreated **(e, f)** replanted teeth 16 weeks post-replantation. Micrographs show optimum microanatomical integration of periodontal progenitor-treated teeth **(a, c, d)** in contrast to resorption, fracture, and partial ankylosis **(b, e, f)** in untreated controls. Individual tissues were labeled for orientation purposes. Levels of tooth displacement in response to mechanical loading **(h)** were very similar between progenitor-treated replants and WT controls, whereas nontreated replants were lost, loose, or ankylosed (respective percentages provided in **g**). CT, computed tomography; cr, crown; res, resorption; rt, root; ab, alveolar bone; de, dentin; ank, ankylosis; cem, cementum.

Throughout their lifetime, tooth periodontia are constantly exposed to a number of biomechanical forces, most frequently as a result of their contact with antagonistic teeth.[27] These forces result in a physiological displacement of teeth and subsequent return to a resting position. To test whether replanted teeth would withstand displacement after application of a physiological bite force, replanted and control teeth were subjected to a displacement test. For this study, forces of 10 and 15 N were applied to the crown surface and displacement was measured using high magnification digital morphometry. Control teeth and progenitor-treated replants showed similar displacement patterns with $141 \pm 23$ μm and $156 \pm 19$ μm displacement after application of 10 N and $297 \pm 34$ μm and $300 \pm 26$ μm displacement after application of 15 N, respectively (Fig. 4h). In contrast, application of 10 or 15 N forces resulted in unlimited displacement of loosely attached teeth in the group that was not pretreated with progenitor cells (Fig. 4h). A comparison with 1 N displacement force resulted in an effective displacement of $626 \pm 31$ μm of loosely attached teeth (Fig. 4h) ($p < 0.005$ in each comparison). Thus, also from a mechanical perspective, our engineered periodontia closely resembled their natural counterparts.

To determine whether newly formed periodontia were generated by progenitor cells used to populate tooth roots before replantation or whether these newly formed tissues had been regenerated through invasion of potent cells from surrounding tissues, progenitor cells were GFP labeled before incubation with denuded tooth roots. Our data demonstrated that GFP-positive mPDLP cells had regenerated the periodontium and formed a firm attachment between the root dentin of the replanted tooth and the alveolar bone at 8 weeks postimplantation (Fig. 5b, c, f, g). In contrast, there was a distinct lack of GFP expression in the noncell-seeded tooth replants and a thin space between the tooth root and fibrous tissue that lacked attachment (Fig. 5a, e). In addition,

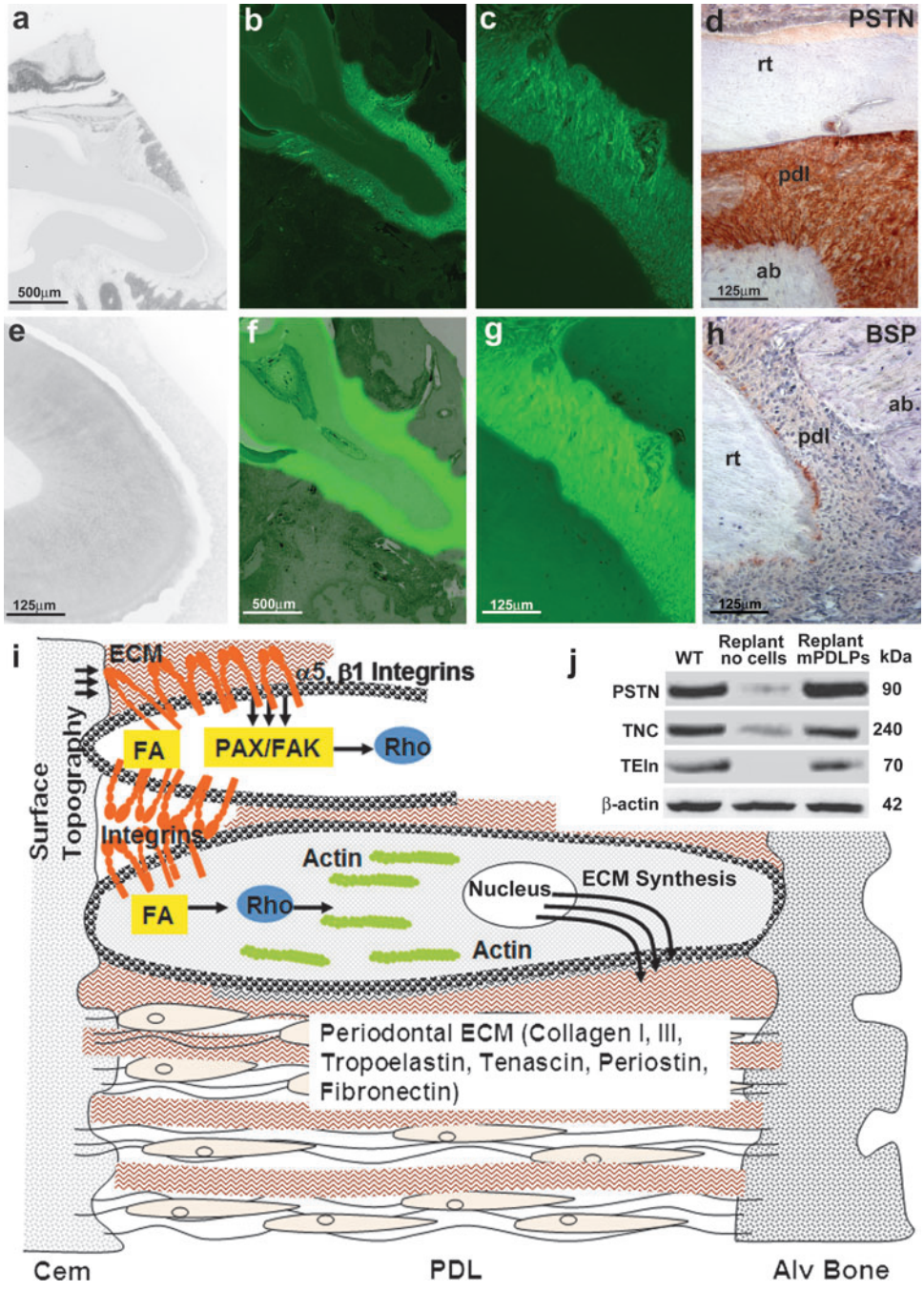


**FIG. 5.** Molecular characterization of the attachment apparatus of replanted teeth by molecular tracing, immunohistochemisty, and Western blotting. Fluorescent micrographs illustrated green fluorescence throughout the entire newly formed PDL **(b, c, f, g)**, whereas there was no fluorescence in nontreated replanted teeth **(a, e)**, suggesting that the newly formed periodontium was formed by GFP-labeled, periodontal progenitors seeded on denuded root surfaces before replantation. **(b, c)** GFP images; **(a, e** and **f, g)** overlays of the respective GFP and phase-contrast images at a magnification of 5×(**a, b, f**; scale bar 500 μm) and 20×(**c, e, g**; scale bar = 125 μm). **(d, h)** Immunohistostains for periostin **(d)** and BSP **(h)** on paraffin sections of mPDLP seeded first maxillary molars that were replanted into the tooth socket and maintained *in vivo* for 8 weeks. **(d)** Note the intense localization of periostin along the newly synthesized PDL fibers as seen in the native PDL. BSP expression was specifically localized at the apical root tip **(h)**. **(j)** Similar expression levels for the ECM proteins PSTN, TNC, and TEIn between the progenitor cell-treated replants and WT controls as demonstrated by Western blot. In contrast, expression levels for these genes in cell-free replants were either low (periostin and tenascin C) or nondetectable (tropoelastin). **(i)** The sketch illustrates a simplified model of the effect of surface topography on periodontal progenitor cell shape and gene expression. Integrin surface receptors feed PDL cells with information about surrounding surfaces via the adhesome gene network. Integrin assembly and signal transduction cascades then affect intracellular machineries, including focal adhesion kinases and paxillins, which in turn regulate GTPases such as Rho to modulate actin microfilament polymerization and associated cytoskeletal changes. These changes cause PDL progenitors to elongate and stretch. In addition, intracellular integrin pathways also affect ECM gene expression, including collagens and periodontal matrix related proteins such as periostin. Thus, through the adhesome and associated integrin receptors, cell surfaces affect both periodontal cell shape and periodontal ECM gene expression, providing tissue-specific control over progenitor fate determination in the periodontal region. ECM, extracellular matrix; TNC, tenascin C; TEIn, tropoelastin; GFP, green fluorescent protein; BSP, bone sialoprotein.

we asked whether newly formed periodontia expressed characteristic periodontal ECM proteins such as periostin, tenascin C, tropoelastin, and BSP (Fig. 5d, h, j). Evaluation by immunohistochemistry and Western blot showed similar protein levels for periostin (130% of WT), tenascin C (92% of WT), and tropoelastin (84% of WT) in WT controls and progenitor-treated replants, whereas expression levels for these proteins in replants that were not incubated with

periodontal progenitors were greatly inhibited (10% for periostin, 21% for tenascin C, and no detectable expression for tropoelastin) (Fig. 5d, h, j), confirming that newly formed periodontia resembled control WT periodontia.

## Discussion and Conclusion

In the present study, we have used the surface-exposed biological tooth root as a template to illustrate the instructive capacity of microstructured apatite surface topography together with the regenerative potential of periodontal progenitor cells to ultimately benefit periodontal regeneration. Our findings indicate that surface topography and progenitor cell type go hand in hand to facilitate optimum periodontal attachment. Microstructures topographies were superior to smooth root surfaces when instructing fiber elongation and focal adhesion gene expression, whereas periodontal progenitors were the most ideally suited progenitor population to favor extension of fibrous ligament cells perpendicular to the root surface. Our data call for the development of optimized materials surface/progenitor combinations as a strategy for organ-specific tissue regeneration.

Our data indicated that periodontal root surface topographies triggered the initiation of classic ECM signaling cascades, starting with the formation of focal adhesions as a materials-induced molecular signaling hub involving integrins and cytosolic mediators and substrates, such as PAX and FAKs.[21,28–31] In our study, levels of phosphorylated PAX, and FAK were elevated as a result of exposure of cells to roughened surfaces. In addition, the prominent PDL cell integrins $\alpha 5$ and $\beta 1$[23,25,26] were also increased in response to microstructured apatite topographies. According to classic integrin signaling pathway routes, focal adhesions activate small GTPases of the Rho family, which in turn directly affect cell shape via the polymerization of actin into F-actin and resulting in stress fibers.[9,32] Our study documented increased levels of Rho A and F-actin, which were both elevated on microstructured root surfaces and in 3D-cultures, pointing to the importance of a three-dimensional environment for proper activation of ECM signaling and regeneration. In addition, tooth root replantation resulted in increased levels of periodontal ECM molecules, including tropoelastin, tenascin, periostin, and fibronectin, suggesting that cells secrete new periodontal ECM in response to physiological forces in the periodontal apparatus (Fig. 5i).

To our knowledge, this is the first progenitor cell-based regeneration of a complete PDL with physiological attachment of a functional tooth. Our strategy could be used for the replantation of teeth lost due to trauma or as a novel approach for tooth replacement using tooth-shaped replicas. Previous studies have succeeded in generating attachment of apatite implants[33] but did not provide convincing evidence for PDL fiber attachment. Others have regenerated a segment of the periodontium after fenestration using a cell sheet engineering strategy.[34,35] However, the origin of newly formed tissues has not been documented in these studies. There has been a first successful report on whole tooth organ replacement,[36] a strategy that still faces significant challenges for clinical application because of difficulties in generating sufficient numbers of suitable progenitor cells. The periodontal progenitors used in the present study can be readily obtained from wisdom teeth, adjacent teeth, or even teeth extracted due to periodontal disease after treatment with inflammatory inhibitors. Future directions of this research may entail microtopographic surface modifications to solid implantable tooth replicas, allowing for the formation of a physiological periodontium that anchors the implanted replica in an alveolar bone socket similar to a natural tooth. From a biological and practical point of view, our microtopography-instructed replantation strategy would be closer within reach than a stem cell-based whole tooth regeneration approach while at the same time mimicking the tactile and biological properties of a physiological periodontium.

## Acknowledgments

Studies were generously supported by the National Institutes of Health Grant DE15045 to T.G.H.D.

## Disclosure Statement

No competing financial interests exist.

## References

1. Tan, W., and Desai, T.A. Microfluidic patterning of cells in extracellular matrix biopolymers: effects of channel size, cell type, and matrix composition on pattern integrity. Tissue Eng **9,** 255, 2003.
2. Norman, J.J., and Desai, T.A. Methods for fabrication of nanoscale topography for tissue engineering scaffolds. Ann Biomed Eng **34,** 89, 2006.
3. Traphagen, S., and Yelick, P.C. Reclaiming a natural beauty: whole-organ engineering with natural extracellular materials. Regen Med **4,** 747, 2009.
4. Matsuura, M., Herr, Y., Han, K.Y., Lin, W.L., Genco, R.J., and Cho, M.I Immunohistochemical expression of extracellular matrix components of normal and healing periodontal tissues in the beagle dog. J Periodontol **66,** 579, 1995.
5. Waddington, R.J., and Embery, G. Proteoglycans and orthodontic tooth movement. J Orthod **28,** 281, 2001.
6. Embery, G. An update on the biochemistry of the periodontal ligament. Eur J Orthod **12,** 77, 1990.
7. Rios, H., Koushik, S.V., Wang, H., Wang, H., Zhou, H.M., Lindsley, A., Rogers, R., Chen, Z., Maeda, M., Kruzynska-Frejtag, A., Feng, J.Q., and Conway, S.J. Periostin null mice exhibit dwarfism, incisor enamel defects, and an early-onset periodontal disease-like phenotype. Mol Cell Biol **25,** 11131, 2005.
8. Rezania, A., and Healy, K.E. Biomimetic peptide surfaces that regulate adhesion, spreading, cytoskeletal organization, and mineralization of the matrix deposited by osteoblast-like cells. Biotechnol Prog **15,** 19, 1999.
9. Giancotti, F.G., and Ruoslahti, E. Integrin signaling. Science **285,** 1028, 1999.
10. Luan, X., Ito, Y., Dangaria, S., and Diekwisch, T.G. Dental follicle progenitor cell heterogeneity in the developing mouse periodontium. Stem Cells Dev **15,** 595, 2006.
11. Wikesjo, U.M., Claffey, N., Christersson, L.A. Franzetti, L.C., Genco, R.J., Terranova, V.P., and Egelberg, J. Repair of periodontal furcation defects in beagle dogs following reconstructive surgery including root surface demineralization with tetracycline hydrochloride and topical fibronectin application. J Clin Periodontol **15,** 73, 1988.
12. Luan, X., Ito, Y., Holliday, S. Walker, C., Daniel, J., Galang, T.M., Fukui, T., Yamane, A., Begole, E., Evans, C., and Diekwisch, T.G. Extracellular matrix-mediated tissue

remodeling following axial movement of teeth. J Histochem Cytochem **55,** 127, 2007.
13. Hynes, R.O. The extracellular matrix: not just pretty fibrils. Science **326,** 1216, 2009.
14. Buser, D., Schenk, R.K., Steinemann, S., Fiorellini, J.P., Fox, C.H., and Stich, H. Influence of surface characteristics on bone integration of titanium implants. A histomorphometric study in miniature pigs. J Biomed Mater Res **25,** 889, 1991.
15. Boyan, B.D., Bonewald, L.F., Paschalis, E.P., Lohmann, C.H., Rosser, J., Cochran, D.L., Dean, D.D., Schwartz, Z., and Boskey, A.L. Osteoblast-mediated mineral deposition in culture is dependent on surface microtopography. Calcif Tissue Int **71,** 519, 2002.
16. Popat, K.C., Daniels, R.H., Dubrow, R.S., Hardev, V., and Desai, T.A. Nanostructured surfaces for bone biotemplating applications. J Orthop Res **24,** 619, 2006.
17. Biggs, M.J., Richards, R.G., McFarlane, S., Wilkinson, C.D., Oreffo, R.O., Dalby, and M.J. Adhesion formation of primary human osteoblasts and the functional response of mesenchymal stem cells to 330 nm deep microgrooves. J R Soc Interface **5,** 1231, 2008.
18. Berrier, A.L., Jones, C.W., and LaFlamme, S.E. Tac-beta1 inhibits FAK activation and Src signaling. Biochem Biophys Res Commun **368,** 62, 2008.
19. Nishiya, N., Kiosses, W.B., Han, J., and Ginsberg, M.H. An alpha4 integrin-paxillin-Arf-GAP complex restricts Rac activation to the leading edge of migrating cells. Nat Cell Biol **7,** 343, 2005.
20. Huttenlocher, A. Cell polarization mechanisms during directed cell migration. Nat Cell Biol **7,** 336, 2005.
21. Geiger, B., Spatz, J.P., and Bershadsky, A.D. Environmental sensing through focal adhesions. Nat Rev Mol Cell Biol **10,** 21, 2009.
22. Giancotti, F.G., and Ruoslahti, E. Elevated levels of the alpha 5 beta 1 fibronectin receptor suppress the transformed phenotype of Chinese hamster ovary cells. Cell **60,** 849, 1990.
23. Ivanovski, S., Komaki, M., Bartold, P.M., and Narayanan, A.S. Periodontal-derived cells attach to cementum attachment protein via alpha 5 beta 1 integrin. J Periodontal Res **34,** 154, 1999.
24. Bolcato-Bellemin, A.L., Elkaim, R., Abehsera, A., Fausser, J.L., Haikel, Y., and Tenenbaum, H. Expression of mRNAs encoding for alpha and beta integrin subunits, MMPs, and TIMPs in stretched human periodontal ligament and gingival fibroblasts. J Dent Res **79,** 1712, 2000.
25. van der Pauw, M.T., Everts, V., and Beertsen, W. Expression of integrins by human periodontal ligament and gingival fibroblasts and their involvement in fibroblast adhesion to enamel matrix-derived proteins. J Periodontal Res **37,** 317, 2002.
26. Kramer, P.R., Janikkeith, A., Cai, Z., Ma, S., and Watanabe, I. Integrin mediated attachment of periodontal ligament to titanium surfaces. Dent Mater **25,** 877, 2009.
27. Nies, M., and Ro, J.Y. Bite force measurement in awake rats. Brain Res Brain Res Protoc **12,** 180, 2004.
28. Discher, D.E, Janmey, P., and Wang, Y.L. Tissue cells feel and respond to the stiffness of their substrate. Science **310,** 1139, 2005.
29. Lim, J.Y., Dreiss, A.D., Zhou, Z., Hansen, J.C., Siedlecki, C.A., Hengstebeck, R.W., Cheng, J., Winograd, N., and Donahue, H.J. The regulation of integrin-mediated osteoblast focal adhesion and focal adhesion kinase expression by nanoscale topography. Biomaterials **10,** 1787, 2007.
30. Saldaña, L., and Vilaboa, N. Effects of micrometric titanium particles on osteoblast attachment and cytoskeleton architecture. Acta Biomater **6,** 1649, 2010.
31. Biggs, M.J., Richards, R.G., and Dalby, M.J. Nanotopographical modification: a regulator of cellular function through focal adhesions. Nanomedicine 2010 [Epub ahead of print].
32. Danen, E.H., Sonneveld, P., Brakebusch, C., Fassler, R., and Sonnenberg, A. The fibronectin-binding integrins alpha5beta1 and alphavbeta3 differentially modulate RhoA-GTP loading, organization of cell matrix adhesions, and fibronectin fibrillogenesis. J Cell Biol **23,** 1071, 2002.
33. Sonoyama, W., Liu, Y., Fang, D. Yamaza, T., Seo, B.M., Zhang, C., Liu, H., Gronthos, S., Wang, C.Y., Wang, S., and Shi, S. Mesenchymal stem cell-mediated functional tooth regeneration in swine. PLoS One **1,** e79, 2006.
34. Nakajima, K., Abe, T., Tanaka, M., and Hara, Y. Periodontal tissue engineering by transplantation of multilayered sheets of phenotypically modified gingival fibroblasts. J Periodontal Res **43,** 681, 2008.
35. Flores, M.G., Yashiro, R., Washio, K. Yamato, M., Okano, T., and Ishikawa, I. Periodontal ligament cell sheet promotes periodontal regeneration in athymic rats. J Clin Periodontol **35,** 1066, 2008.
36. Ikeda, E., Morita, R., Nakao, K., Ishida, K., Nakamura, T., Takano-Yamamoto, T., Ogawa, M., Mizuno, M., Kasugai, S., and Tsuji, T. Fully functional bioengineered tooth replacement as an organ replacement therapy. Proc Natl Acad Sci USA **106,** 13475, 2009.

Address correspondence to:
*Thomas G.H. Diekwisch, D.M.D., Ph.D. (sc.), Ph.D. (phil.)*
*Brodie Laboratory for Craniofacial Genetics*
*University of Illinois at Chicago*
*801 South Paulina*
*Chicago, IL 60612*

*E-mail:* tomdkw@uic.edu

*Received: April 29, 2010*
*Accepted: August 25, 2010*
*Online Publication Date: September 30, 2010*